ChemComm

COMMUNICATION

View Article Online
View Journal | View Issue

Cite this: *Chem. Commun.*, 2025, **61**, 2341

Received 28th September 2024,
Accepted 6th January 2025

DOI: 10.1039/d4cc05070c

rsc.li/chemcomm

Crafting tailored, well-defined block copolymers of cyclic esters with an organomagnesium initiator†

Priyanku Nath, ‡[a] Shweta Sagar, ‡[a] Aranya Ray, [a] Himadri Karmakar, [a] Alok Sarkar, *[b] Vadapalli Chandrasekhar *[c] and Tarun K. Panda *[a]

An organomagnesium complex containing an imino-phosphanamidinate ligand was found to be a competent catalyst for the ROP of *rac*-LA and ε-CL as well as their copolymerization *via* sequential addition of monomers, resulting in the formation of PCL-*b*-PLA diblock copolymer. The polymers obtained were characterized by ^{1}H, ^{13}C, DOSY NMR, DSC, TGA, POM, and SEM.

Aliphatic polyesters present many attractive attributes as they can be made using resources produced from renewable biomass in comparison to petroleum-feed stock based polymers.[1] Among the aliphatic polyesters, polylactides (PLAs) and polycaprolactones (PCLs) have attracted considerable interest.[2] Ring-opening polymerization (ROP) of cyclic esters promoted by organometallic catalysts is the most effective method for preparing polyesters with a well-controlled molar mass, narrow molecular weight dispersity, and precise control over stereoselectivity[3] under mild reaction conditions.

Even though PLAs and PCLs have favorable characteristics each of them possesses certain limitations. Thus, while PLA has good mechanical strength,[4] it suffers from poor elasticity,[4] and brittleness.[4] On the other hand, PCL possesses good elasticity[5] and poor mechanical characteristics.[5] By copolymerizing LA with ε-CL it may be possible to prepare polymers where the complementary strengths of individual homopolymers may be incorporated. Such copolymers have received significant attention in the pharmaceutical and biomedical fields.[6] One such example is the block copolymerization of ε-CL and LA, which allows the excellent permeability of the PCL to be combined with the rapid biodegradation of PLA.[7] The properties of the materials can be fine-tuned by controlling the composition and distribution of the two comonomers in the polymer chain to meet specific requirements in various applications.[8] Because of this importance, developing metal catalysts as effective initiators for the ROP and ROCOP (ring-opening copolymerization) of cyclic esters has received growing attention in recent years. Sn(II)-2-ethyl hexanoate is used on an industrial scale but suffers from toxicity issues, as it is practically impossible to fully remove the tin from the polyesters, thus making such polymers unfit for biomedical applications.[9] Therefore, there is a necessity for the development of biocompatible and non-toxic metal catalysts to make the polymers viable for such applications. Several organometallic compounds involving aluminum,[10] calcium,[11] zinc,[12] magnesium,[13] titanium,[14] and lanthanides,[15] have been successfully used for initiating the ROP of lactones and lactides.

Alkaline earth metals (Mg, Ca, Sr) are suitable alternatives because of their non-toxicity, cost-effectiveness, and compatibility with biological systems. The main challenge in developing these catalysts is that they undergo Schlenk-type equilibria mechanism.[16] In 2022, our group reported a Mg complex supported by flexible amidophosphine chalcogenide and studied its catalytic performance in the isoselective synthesis of PLA and PCL without any external initiator, but it could not initiate ROCOP.[17] Consequently, we were keen to develop novel initiators that are active in ROCOP that enable a statistical distribution of comonomer subunits in the polymer chain. Looking into the literature, limited Mg complexes have been studied for ROCOP of rac-LA and ε-CL producing block copolymers (PCL-*b*-PLA).[18–20] However, these catalysts typically require an external initiator/cocatalyst to initiate the ROP. We recently reported an imino-phosphanamidinate-supported Cs complex enabling efficient ROP and ROCOP of *rac*-LA and ε-CL in the absence of an external initiator.[21] To further continue our efforts toward designing novel catalysts, we have synthesized

[a] *Department of Chemistry, Indian Institute of Technology Hyderabad, Kandi – 502 284, Sangareddy, Telangana, India. E-mail: tpanda@chy.iith.ac.in*
[b] *Momentive Performance Materials Pvt. Ltd., Survey No. 09, Hosur Road, Electronic City (west), Bangalore-560100, India*
[c] *Tata Institute of Fundamental Research Hyderabad, Gopanpally, 500107, Hyderabad, India. E-mail: vc@tifrh.res.in*

† Electronic supplementary information (ESI) available: For experimental details and characterization through NMR, GPC, DSC, TGA. CCDC 2387519. For ESI and crystallographic data in CIF or other electronic format see DOI: https://doi.org/10.1039/d4cc05070c

‡ Equal contribution.

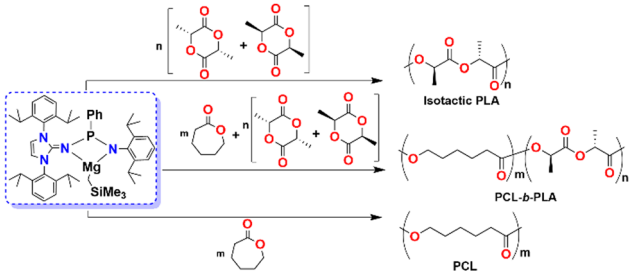

Fig. 1 Mg complex as catalyst for ROP and ROCOP of cyclic esters in this work.

an imino-phosphanamidinate-supported Mg complex (**1**). The present work describes the synthesis and the application of the imino-phosphanamidinate-supported Mg complex (**1**) as a competent catalyst in the ROP and ROCOP of *rac*-LA and ε-CL without any external initiator (Fig. 1).

Complex **1** was synthesized by the reaction of imino-phosphanamidinate ligand with $Mg(CH_2SiMe_3)_2$ to yield the Mg alkyl complex [κ²-{NHI^{Dipp}P(Ph)*N*-Dipp}$MgCH_2SiMe_3$] (Scheme 1). Complex **1** was characterized thoroughly using multinuclear NMR spectroscopy and single-crystal X-ray crystallography. The molecular structure of **1** in the solid state is furnished in Fig. 2. The Mg^{2+} ion is bonded to two nitrogen atoms (N3 and N4) from the monoanionic imino-phosphanamide [NHI^{Dipp}P (Ph)N^{dipp}]$^-$ moiety and one neosilyl group. Important metrical parameters of the complex are summarized in the caption of Fig. 2. When complex **1** was initially investigated, the ROP of *rac*-LA was performed without an external initiator (Table S11 in ESI†). The polymerization of *rac*-LA with a monomer-to-catalyst ratio of 100 : 1 was accomplished

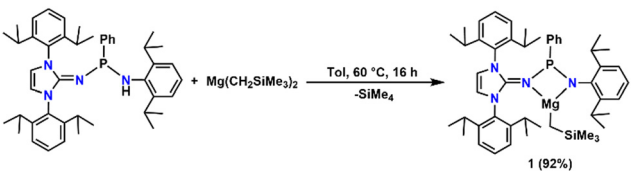

Scheme 1 Synthesis of magnesium alkyl complex (**1**) supported by imino-phosphanamidinate ligand.

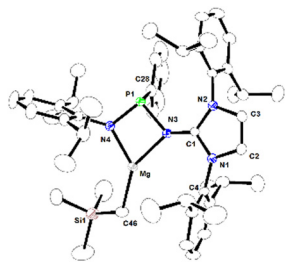

Fig. 2 The molecular structure of Mg-complex 1 with the thermal displacement parameters drawn at 30% probability. Hydrogen atoms are omitted for clarity. Selected bond lengths [Å] and bond angles [°]: Mg–N4 1.9922(16), Mg–N3 2.0832(14), Mg–C46 2.100(9), P1–N4 1.6732(14), P1–N3 1.7607(14), C46–Si1 1.786(9), N3–P1–N4 92.34(7), N3–Mg–N4 74.86(6), N4–Mg–C46 136.2(3), N3–Mg–C46 144.9(4), P1–N4–Mg 99.26(7), P1–N3–Mg 93.14(6), Mg–C46–Si1 116.2(6). CCDC No. 2387519.

with 97.1% conversion within 6 h at 90 °C in toluene (Table S11, entry 1, ESI†). However, using **1** as the catalyst, the same reaction took six hours to achieve 50% monomer conversion when THF was used as a solvent (Table S11, entry 6, ESI†). The reason for the variation in reaction rates is due to the competitive coordination between solvents with different polarities and THF with active metal centers, reducing the LA-metal interaction. Therefore, toluene was selected as the ideal solvent to reduce solvent influence in the ROP of LA. When we increased the quantity of the monomer up to 400 equivalents of *rac*-LA with **1** as the catalyst in toluene for 6 h, the conversion observed was 71.4%, affording a molecular weight of 39.7 kDa and dispersity (*Đ*) around 1.5. The molecular weights of the polymers (M_n) agreed well with their calculated values and showed a linear relationship (Fig. S16 in ESI†), with an increase in the quantity of the monomer, and the narrow molecular weight distributions were confirmed by GPC analysis. This linear relationship between ($M_{n,exp}$) determined by GPC and calculated molecular weights ($M_{n,theo}$) indicates a living polymerization process. Furthermore, this suggests that the polymerization process was effectively well-controlled, exhibiting a high initiation efficiency when the Mg complex was used as an initiator. The Mg complex showed good control in polymer stereoselectivity and produced isotactic-rich polymers, confirmed by the homonuclear decoupled ^{1}H NMR spectrum (Fig. S21 in ESI†). The high tetrad intensity of *mmm* suggests that monomers with the same stereochemical configurations are significantly more common throughout the polymer chain. The P_i values of 0.85, 0.79, 0.75, and 0.73 were achieved when the stoichiometric ratios of [LA] : [**1**] were varied in the order of 100 : 1, 200 : 1, 300 : 1, and 400 : 1, respectively. The thermal analysis of a representative PLA sample with P_i = 0.85 *via* differential scanning calorimetry (DSC) displayed a glass transition peak (T_g) at 60.7 °C and a melting peak (T_m) at 205.6 °C (Fig. S22 in ESI†).[22] The sample was also analyzed by thermogravimetric analysis (TGA), which ensured high thermal stability of the synthesized PLA up to 234.10 °C (Fig. S23 in ESI†).

A typical kinetics study was conducted to determine the reaction order with respect to the monomer and catalyst (refer to ESI,† for details). The kinetic plots for $[LA]_0/[LA]$ *vs.* [cat **1**] were found to be linear, which indicates that there is a first-order dependence on *rac*-LA concentration (Fig. S4 in ESI†). Since the polymerization reactions showed first-order dependence, it validates the presence of only one initiator. The activation parameters for the ROP or *rac*-LA in $CDCl_3$ were found to be $\Delta H^{\ddagger}$ = 20.2 kJ mol^{-1} and $\Delta S^{\ddagger} = -238.6$ J (mol K)$^{-1}$, $\Delta E_a^{\ddagger} = 23.2$kJmol^{-1}. A $\Delta G^{\ddagger}$ value of 106.8 kJ mol^{-1} was calculated for the ROP of *rac*-LA catalyzed by the catalyst **1** at 90 °C (Fig. S8 and S9 in ESI†). We also carried out reactions in the presence of external initiators like benzyl alcohol (BnOH), where we observed that the ROP rate was practically the same for most cases (Fig. S11 in ESI†). Further, reactions were performed by varying the concentrations of BnOH and keeping the catalyst **1** concentration and *rac*-LA constant. However, in all cases, the value of the rate constant k_{obs} remains the same. This lack of dependence on BnOH concentration confirms its zero-order contribution to the rate law (Fig. S14 and S15 in ESI†). Further, the *in situ* characterization of the active

catalyst species using the ^{1}H NMR technique revealed the coordination and the attachment of growing polymer chains with the Mg complex (Fig. S40, ESI†). The outcome results demonstrated that the polymerization continued *via* a so-called "coordination-insertion mechanism" which is renowned for most alkali metal phenoxides systems where the *rac*-LA was first activated after coordination to the metal centers and then ring-opened *via* nucleophilic attack by the lone pair of N atom of P–N bond. Based on the above information, a plausible mechanism is proposed (Fig. S41, ESI†).

Complex **1** was also examined for the activity as an initiator for the ROP of ε-CL without any external initiator. Reaction details are summarized in (Table S13 in ESI†). Overall, the ROP process had good control, allowing PCLs with a significant match between $M_{n,theo}$ and $M_{n,exp}$, with $Đ$ up to 1.3 as determined by GPC. A linear relationship for both $M_{n,theo}$ and $M_{n,exp}$ *versus* [ε-CL]:[**1**] ratio further validates chain-end controlled living polymerization with minimum side reactions (Fig. S29 in ESI†). The thermal properties of the polymer obtained were determined by DSC and TGA analysis. The TGA thermogram of the synthesized PCL showed its thermal stability up to 283.07 °C (Fig. S28 in the ESI†). The melting points of the synthesized PCL by DSC were noted to be at 61.5 °C and 63.6 °C for the M_n value of 10.1 kDa and 31.4 *k*Da, respectively (Fig. S27 in the ESI†).

For complex **1**, we initially attempted to polymerize *rac*-LA followed by ε-CL addition; we could observe no incorporation of ε-CL into the polymer chain. However, the desired copolymer was obtained when we changed the sequence to polymerize ε-CL to PCL, followed by the addition of *rac*-LA. The obtained copolymers showed monomodal molecular weight distributions, with a good agreement between the experimental and theoretical molecular weights. We performed a series of copolymerization reactions of *rac*-LA and ε-CL with [LA]:[CL]:[**1**] ratio of 50/50/1 at different times using toluene as a solvent, as mentioned in Table 1. Initially, monomer conversions of 88.9% for ε-CL and 76.7% for *rac*-LA were achieved within 6 h, producing a copolymer with 59.4% caproyl and 40.6% lactidyl units, which resulted in a copolymer with a caprolactone enriched composition (Table 1, entry 1). On increasing the reaction time up to 12 h, the copolymer composition with lactidyl units increased to 47.1% and decreased to 52.5% for caproyl units. After 24 h, under the same conditions, monomer conversions reached more than 90%, producing a copolymer with 50.9% caproyl and 49.1% lactidyl units, resulting in almost 50 : 50 inclusion of LA and CL (Table 1, entry 3). We were also interested in regulating the feed ratio of the monomers; as a result, subsequent copolymerization reactions were conducted, varying the feed ratios of CL to LA but maintaining constant catalyst loadings (40 : 60 and 60 : 40). For both ratios, di-block copolymers were produced with comonomer ratios integrated into the polymer chains confirmed by ^{1}H and ^{13}C NMR spectroscopy. From the ^{1}H NMR spectrum (Fig. 3), the signals for the methylene protons (–CH_2–OH) of the hydroxyl end groups of the PCL polymers at 3.57 ppm disappeared completely in the isolated polymer, and we observed a new signal at 4.29 ppm, which corresponds to the methine proton [–$CH(CH_3)$OH] of the hydroxyl end group in the copolymer. From this observation, we can conclude that the polymerization of LA was initiated by the PCL reactive chain end.[14] While analyzing PCL's methylene signal in the ^{1}H NMR spectrum, we observed a triplet at δ 2.33 ppm, and CL–LA linkage was observed at δ 2.36 ppm. The ^{13}C NMR spectra (Fig. S31 in ESI†) exhibited two peaks at 169.6 ppm and 173.5 ppm, corresponding to lactidyl C═O sequences and caproyl C═O sequences.[23] No additional signals were observed between the two signals, indicating no transesterification occurred during the copolymerization.[23] The GPC analysis further confirmed the presence of copolymers through an increase in M_n and a monomodal peak for the PCL-*b*-PLA copolymer (Fig. S34 in ESI†). The formation of a copolymer was also supported by DOSY NMR (Fig. S35 in ESI†), as a single diffusion coefficient was observed for both PCL and PLA resonances. The structures of the PCL/PLA copolymers can be determined by measuring the ratio of the signal of polymerized CL linked to the LA molecule to the signal of terminal LA in the ^{1}H NMR.[20] The value for the copolymer sample was near 1, indicating that a di-block copolymer structure had been exclusively formed. The randomness factor, *R*, gives insight into whether the copolymer has a well-defined block structure (R = 0) or a pure random structure (R = 1, refer to ESI†).[24] For the copolymers, the *R* values range from 0.02–0.03, confirming the formation of block

Table 1 Block copolymerization of ε-CL and *rac*-LA using catalyst **1**[a]

Run	[CL]:[LA]:[1]	Time (h) CL	Time (h) *rac*-LA	CL/LA[b] Conv (%)	CL/LA[c] (mol %)	Ratio of CL/LA: terminal LA[d]	R[e]	$M_{n,theo}$[f] (*k*Da)	$M_{n,NMR}$ (*k*Da)	$M_{n,exp}$[g] (*k*Da)	$Đ$[g]
1	50 : 50 : 1	2	6	88.9/76.7	59.4/40.6	0.67	0.02	12.9	10.5	6.1	1.2
2	50 : 50 : 1	2	12	90.1/80.6	52.5/47.1	0.98	0.02	12.9	10.9	7.7	1.2
3	50 : 50 : 1	2	24	96.3/90.1	50.9/49.1	1	0.02	12.9	12.1	12.5	1.3
4	40 : 60 : 1	2	24	93.4/89.9	39/60.1	0.75	0.01	14.3	11.8	10.5	1.4
5	30 : 70 : 1	2	24	95.7/87.3	33/66	0.99	0.02	13.5	11.7	9.8	1.1
6	60 : 40 : 1	2	24	90.3/72.1	76.3/23.7	0.88	0.03	12.6	10.3	9.5	1.2

[a] Reaction conditions: Tol (4 ml), 90 °C. [b] Percentage conversion of the monomer determined by ^{1}H NMR spectroscopy in $CDCl_3$. [c] CL/LA mole ratio in copolymer. [d] Determined from ^{1}H NMR integrals for purified copolymer samples. [e] Randomness factor, *R*: R = 0 (blocky structure), R = 1 (fully random). [f] $M_{n,theo}$ = ([CL]/[1] × % CL × 114.14) + ([LA]/[1] × % LA × 144.13) + 32 (for end group). [g] Determined by GPC relative to polystyrene standards in tetrahydrofuran: M_n (GPC) = M_n (GPC) × CL (% mol in copolymer) × 0.56 + M_n (GPC) × LA (% mol in copolymer) × 0.58. Universal calibration was carried out using polystyrene standards, laser light scattering detector data, and a concentration detector. Each experiment is duplicated to ensure precision.

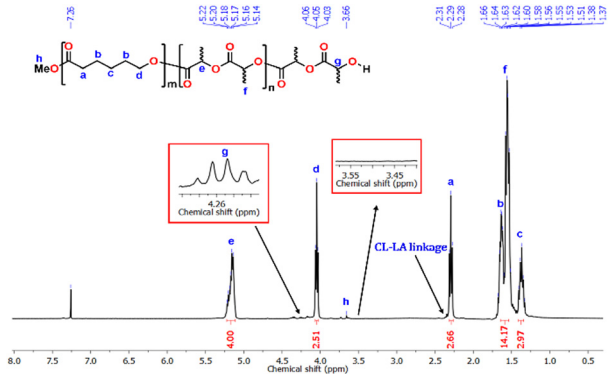

Fig. 3 ^{1}H NMR spectrum of a PCL-*b*-PLA copolymer (Table 1, entry 4).

copolymers. Thermal analysis of the copolymers (PCL-*b*-PLA) was carried out by DSC and showed two T_m at 60.3 °C for the PCL block and 237.8 °C for the PLA block (Fig. S36 in ESI†). From the TGA analysis, copolymer exhibited a two-step degradation where the first step at 246.80 °C can be ascribed to the degradation of PLA, and the second one at 412.16 °C can be ascribed to the degradation of PCL portions (Fig. S37 in ESI†).[25] Notably, complex **1** also displays stereocontrol for *rac*-LA ROP, resulting in isotactic PLA blocks (Fig. S42 in ESI†).

Further, the SEM analysis of the copolymers indicated that both PLA and PCL segments exhibited different morphologies due to microscopic phase separation.[26] Sample with equal proportion of PCL and PLA (50.9 : 49.1%) is composed of a continuous fractured surface for PLA and droplet matrix morphology for PCL segment. Upon increasing the PCL content to 76.3%, an increase in droplet matrix morphology with a relatively larger spherical droplet was observed. The optical microscopic analysis of the copolymer sample (entry 6 and 4) showed formation of spherulites of PCL segment uniformly distributed throughout the amorphous PLA matrix.

In conclusion, the Mg imino-phosphanamidinate complex was able to initiate the ROP of *rac*-LA and ε-CL in a controlled manner and the formation of a well-defined block copolymer of PCL-*b*-PLA *via* sequential addition of monomers with controlled molecular weight distribution and narrow dispersity. To the best of our knowledge, this is the first example of a single-site imino-phosphanamidinate supported magnesium catalyst for ROP of *rac*-LA and ε-CL as well as their copolymerization to form PCL-*b*-PLA diblock. The PLAs produced using this catalyst show an isoselectivity of 0.85 which is the highest to date by magnesium complex without using any external initiator. The polymer samples were characterized by ^{1}H and ^{13}C, DOSY NMR, DSC, POM, and SEM. This work will encourage researchers to develop Mg complexes that could be utilized to synthesize biodegradable polymers with good selectivity.

P. N. and H. K. express gratitude to CSIR (09/1001(15565)/2022-EMR-I and (09/1001(0038)/2018-EMR-I) and S. S. Thanks to PMRF (2000829) and A. R. thanks to DST-INSPIRE (IF230098) India for their PhD fellowships. Financial support from SERB, India under project no. CRG/2022/001941 is appreciated. We thank Rohan K. Meher for his assistance with the TOC graphic.

Data availability

The data supporting this article have been included as part of the ESI.†

Conflicts of interest

There are no conflicts to declare.

References

1 M. A. Hillmyer and W. B. Tolman, *Acc. Chem. Res.*, 2014, **47**, 2390–2396.
2 M. J. L. Tschan, E. Brulé, P. Haquette and C. M. Thomas, *Polym. Chem.*, 2012, **3**, 836–851.
3 Y. Sarazin and J. F. Carpentier, *Chem. Rev.*, 2015, **115**, 3564–3614.
4 S. Farah, D. G. Anderson and R. Langer, *Adv. Drug Delivery Rev.*, 2016, **107**, 367–392.
5 B. N. Mankaev, V. A. Serova, M. U. Agaeva, K. A. Lyssenko, A. N. Fakhrutdinov, A. V. Churakov, E. V. Chernikova, M. P. Egorov and S. S. Karlov, *J. Organomet. Chem.*, 2024, **1005**, 122973.
6 D. J. Darensbourg and O. Karroonnirun, *Macromolecules*, 2010, **43**, 8880–8886.
7 L. Qin, J. Bai, Y. Zhang and X. Chen, *J. Organomet. Chem.*, 2018, **871**, 40–47.
8 G. Li, M. Lamberti, D. Pappalardo and C. Pellecchia, *Macromolecules*, 2012, **45**, 8614–8620.
9 A. C. Albertsson and I. K. Varma, *Biomacromolecules*, 2003, **4**, 1466–1486.
10 S. Sagar, P. Nath, K. Bano, H. Karmakar, J. Sharma, A. Sarkar and T. K. Panda, *ChemCatChem*, 2024, **16**, e202300972.
11 J. Bhattacharjee, A. Harinath, A. Sarkar and T. K. Panda, *Chem. – Asian J.*, 2020, **15**, 860–866.
12 J. E. Chellali, A. K. Alverson and J. R. Robinson, *ACS Catal.*, 2022, **12**, 5585–5594.
13 P. McKeown, S. N. McCormick, M. F. Mahon and M. D. Jones, *Polym. Chem.*, 2018, **9**, 5339–5347.
14 D. Dakshinamoorthy and F. Peruch, *J. Polym. Sci., Part A: Polym. Chem.*, 2012, **50**, 2161–2171.
15 W. Gu, P. Xu, Y. Wang, Y. Yao, D. Yuan and Q. Shen, *Organometallics*, 2015, **34**, 2907–2916.
16 J. S. Alexander and K. Ruhlandt-Senge, *Eur. J. Inorg. Chem.*, 2002, 2761–2774.
17 S. Sagar, K. Bano, A. Sarkar, K. Pal and T. K. Panda, *Eur. J. Inorg. Chem.*, 2022, e202200494.
18 M. Slattery, A. E. Stahl, K. R. Brereton, A. L. Rheingold, D. B. Green and J. M. Fritsch, *J. Polym. Sci., Part A:Polym. Chem.*, 2019, **57**, 48–59.
19 T. Rosen, I. Goldberg, W. Navarra, V. Venditto and M. Kol, *Angew. Chem.*, 2018, **130**, 7309–7313.
20 M. A. Rahman, T. J. Neal and J. A. Garden, *Chem. Commun.*, 2024, **60**, 5530–5533.
21 S. Sagar, H. Karmakar, P. Nath, A. Sarkar, V. Chandrasekhar and T. K. Panda, *Chem. Commun.*, 2023, **59**, 8727–8730.
22 K. Fukushima and Y. Kimura, *Polym. Int.*, 2006, **55**, 626–642.
23 L. Peponi, A. Marcos-Fernández and J. M. Kenny, *Nanoscale Res. Lett.*, 2012, **7**, 103–110.
24 J. Fernandez, A. Etxeberria and J.-R. Sarasua, *J. Mech. Behav. Biomed. Mater.*, 2012, **9**, 100–112.
25 J. Contreras, J. Pestana, F. López-Carrasquero and C. Torres, *Polym. Bull.*, 2014, **71**, 1661–1674.
26 A. S. Luyt and S. Gasmi, *J. Mater. Sci.*, 2016, **51**, 4670–4681.

